Supplementary Information (SI) for Analytical Methods.
This journal is © The Royal Society of Chemistry 2026

Real-Time Resonance Raman Spectroscopic Monitoring of the Briggs-Rauscher Reaction

(Supplementary Information)

Clark D. Gray[1], Nigel Gotts[1], Casassio Lima[1], Kenneth Williams[2], Sebastien Maussang[2], Royston Goodacre[1*]

[1]Centre for Metabolomics Research, Department of Biochemistry, Cell and Systems Biology, Institute of Systems, Molecular and Integrative Biology, University of Liverpool, BioSciences Building, Crown St., Liverpool, UK, L69 7ZB.

[2] Renishaw plc, Spectroscopy Products Division, New Mills, Kingswood, Wotton-under-Edge GL12 8JR.

*correspondence to : Professor Royston Goodacre (roy.goodacre@liverpool.ac.uk).

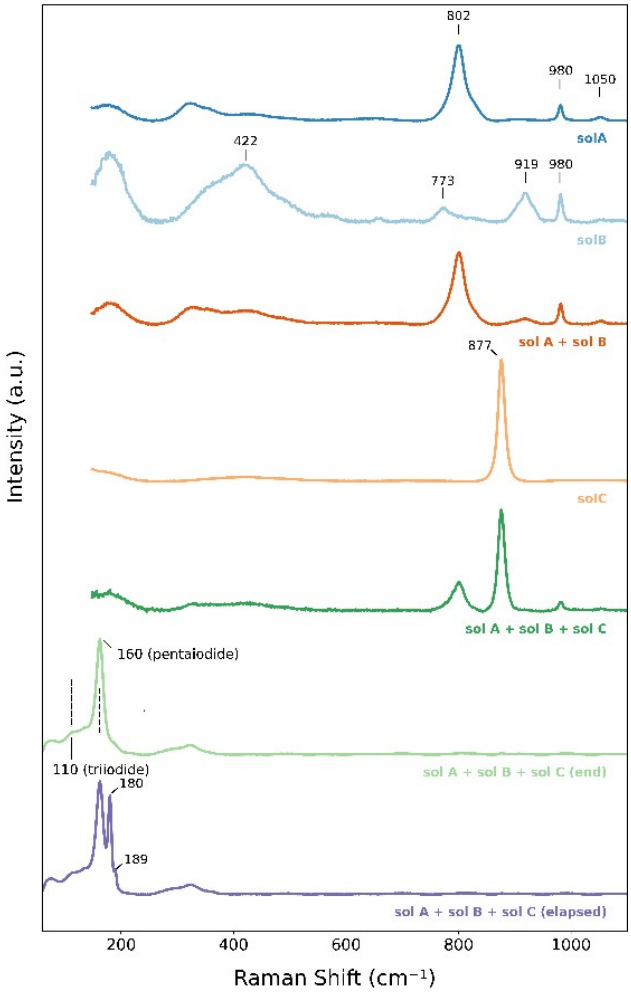

Figure S1: Raman spectra of solution A, solution B, solution C as well as their intermediary mixture and subsequent polyiodide spectrum. Solution A, B and C were acquired with10 s exposure time over 9 s accumulations. The intermediary was acquired by accumulating 12 spectra in the intermediary phase. The end spectra were acquired by accumulating 161 spectra after the colour change had taken place. The elapsed spectra were acquired by accumulating 276 spectra after the spectra had reached a maximum. All spectra had their cosmic rays removed, were subsequently smoothed using Savitzky–Golay filtering, were baselined using Asymmetric Least Squares, and were finally normalised and scaled.

Table S1: Table of solution and dissolved compounds with Raman assignments as per Figure S2.

Solution	Contains	Assignments
A	• Potassium iodate (43 g, 200mM) • Sulfuric acid (4.5 mL, 45 mM).	802 cm^{-1} : I–O bending, trigonal pyramidal structure of the IO_3^- anion. [3] 980 and 1050 cm^{-1}: symmetric and asymmetric modes of SO_4^{2-}. [1, 2]
B	• Malonic acid (15.6 g, 150 mM) • Manganese sulphate monohydrate (3.04 g, 20 mM) • Starch (0.4 g, 220 mM).	980 cm^{-1}: manganese sulphate monohydrate. 422 cm^{-1} : HSO_4^-. [1] 773 cm^{-1} : O=C-O deformation, 919 cm^{-1} : C-C chain vibrations. [4]
C	• Hydrogen peroxide (350 mL, 3.08 M).	877 cm^{-1} : O–O stretching mode in hydrogen peroxide. [5]

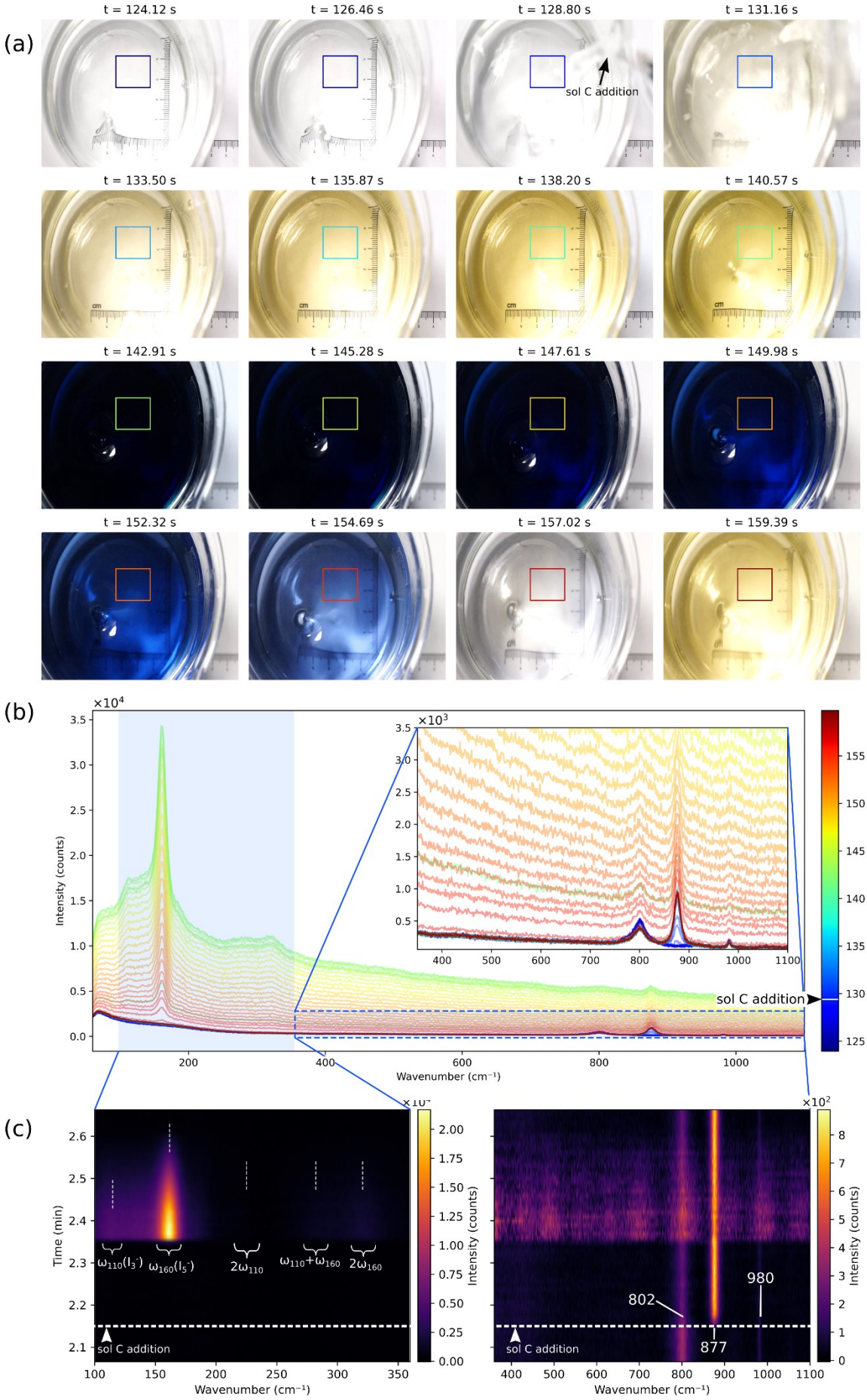
(a)
t = 124.12 s
t = 126.46 s
t = 128.80 s
sol C addition
t = 131.16 s
t = 133.50 s
t = 135.87 s
t = 138.20 s
t = 140.57 s
t = 142.91 s
t = 145.28 s
t = 147.61 s
t = 149.98 s
t = 152.32 s
t = 154.69 s
t = 157.02 s
t = 159.39 s
(b)
×10^4
Intensity (counts)
×10^3
Wavenumber (cm⁻¹)
Time (s)
sol C addition
(c)
Time (min)
ω110(I3-)
ω160(I5-)
2ω110
ω110+ω160
2ω160
sol C addition
Wavenumber (cm⁻¹)
Intensity (counts)
×10^2
980
802
877
sol C addition
Wavenumber (cm⁻¹)
Intensity (counts)

Figure S2: A single Briggs–Rauscher cycle following the addition of solution C. (a) 16 evenly time spaced camera frames, with the boxed region indicating the pixel area used for HSV-luminosity analysis. (b) Time-series in situ Raman spectra showing the transition from solutions A + B through the addition of solution C to the subsequent rapid polyiodide formation. (c) In situ Raman spectra (smoothed, baselined): left—overall polyiodide growth; right—autoscaled 400–1100 cm^{-1} region highlighting the emergence of the 877 cm^{-1} H_2O_2 band, with the 802 and 980 cm^{-1} modes remaining constant.

Weighted Moving Average (WMA)

WMA was employed with a bin span of 3. This Python script for this processing step is available on GitHub as wma_smoothing.py.

Video and Raman Data Correspondence

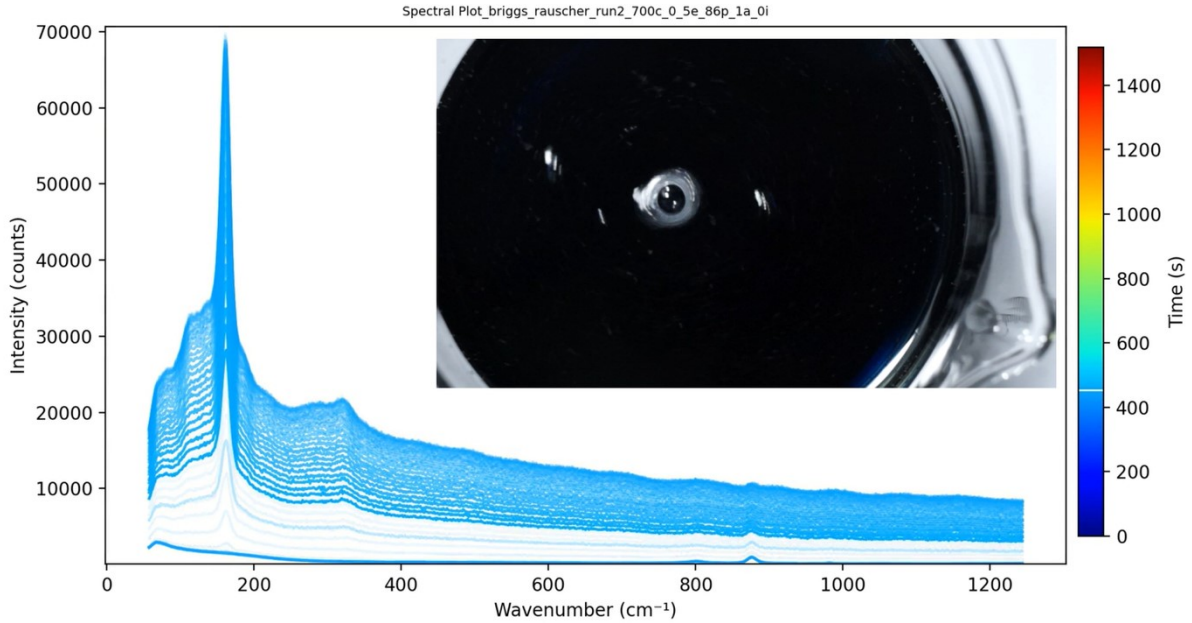

Figure S3: Video screenshot of Raman data alongside video footage of reaction. Full video may be found in briggs_rauscher_run4_700c_0_5e_86p_1a_0i_baseline_l3.0_p5.0_animation_real_time_with_visual_side.mp4

The video and Raman data may be played side by side in briggs_rauscher_run4_700c_0_5e_86p_1a_0i_baseline_l3.0_p5.0_animation_real_time_with_visual_side.mp4

Investigating malonic acid variation effects

Furrow and Noyes demonstrate the importance of malonic acid as the best organic acid in the reaction through substitution of other organic acids. [6] At 0.2 M of $CH_2(COOH)_2$ the I_2 is consumed to produce I^-, turning the solution to clear, and ending the reaction cycle (see Figure S4). This is further event by the higher frequency of BR reactions with 0.25M than with 0.1 M and 0.15 M of malonic acid.

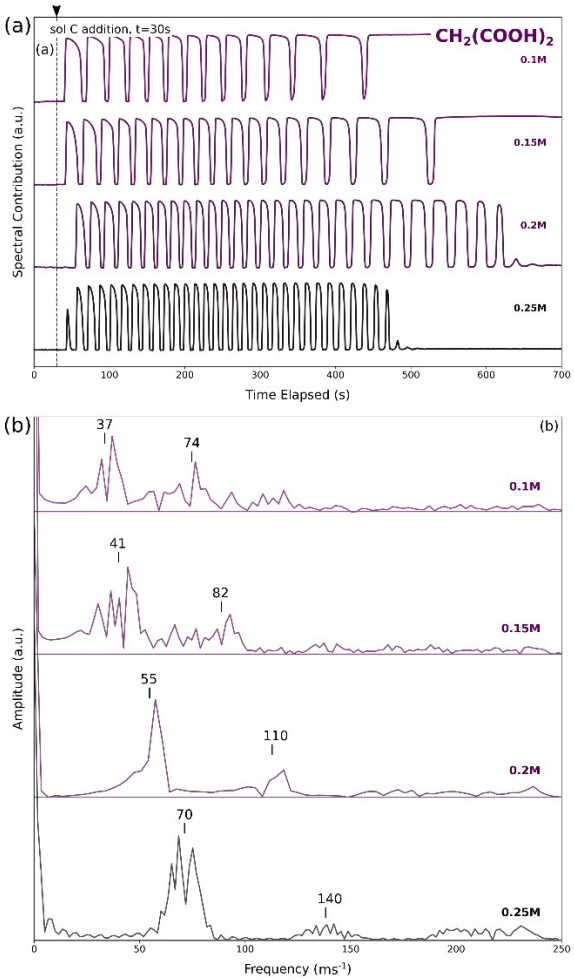

Figure S4: $CH_2(COOH)_2$ -dependent DCLS spectral contributions following the addition of solution C at (t = 30 s). (a) Time-resolved DCLS signals showing variation in oscillatory behaviour with changing $CH_2(COOH)_2$ concentration. (b) Corresponding FFT spectra showing changes in frequency and spectral features with varying $CH_2(COOH)_2$ concentration. Investigating potassium iodate variation effects.

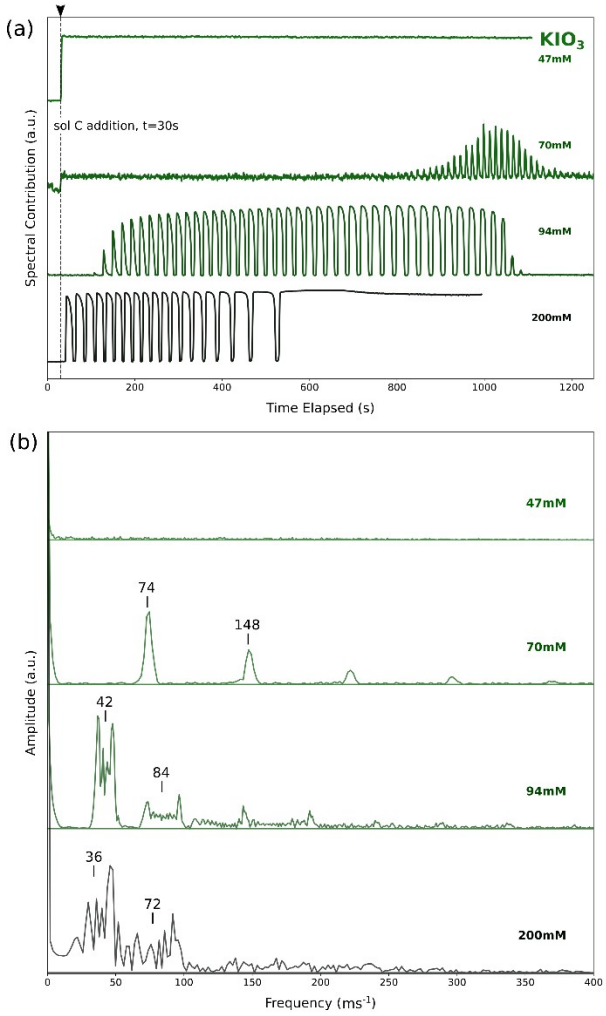

Figure S5: KIO_3-dependent DCLS spectral contributions following the addition of solution C at (t = 30 s). (a) Time-resolved DCLS signals showing variation in oscillatory behaviour with changing KIO_3 concentration, showing no oscillations at 47nM. (b) Corresponding FFT spectra showing changes in frequency and spectral features with varying KIO_3 concentration.

Upon depletion of the BR oscillations, the elevated intensity in background and resonance modes arising from polyiodide production obscures the Raman signatures associated with IO_3^-, complicating subsequent spectroscopic analysis.

Investigating hydrogen peroxide variation effects

Raman spectroscopic data of 0.44M, 0.88M, and 1.76M of H_2O_2 reveal the decrease of the 877 cm^{-1} band of the O–O stretching mode. The decrease in the 877 cm^{-1} mode corresponds with the sudden disruption of the oscillations (see Figure S6). Therefore, the presence H_2O_2 is vital for sustaining the oscillatory reaction, namely inducing the initial oxidation reaction for I_2 production.

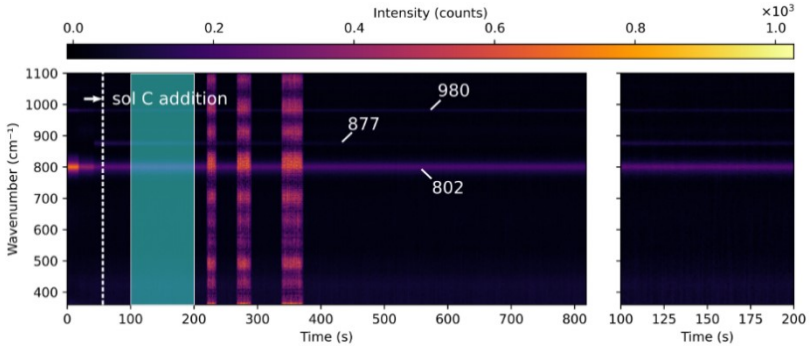

Figure S6: Time-matched in situ Raman spectroscopic time-series BR reaction at H_2O_2 of 0.44M.

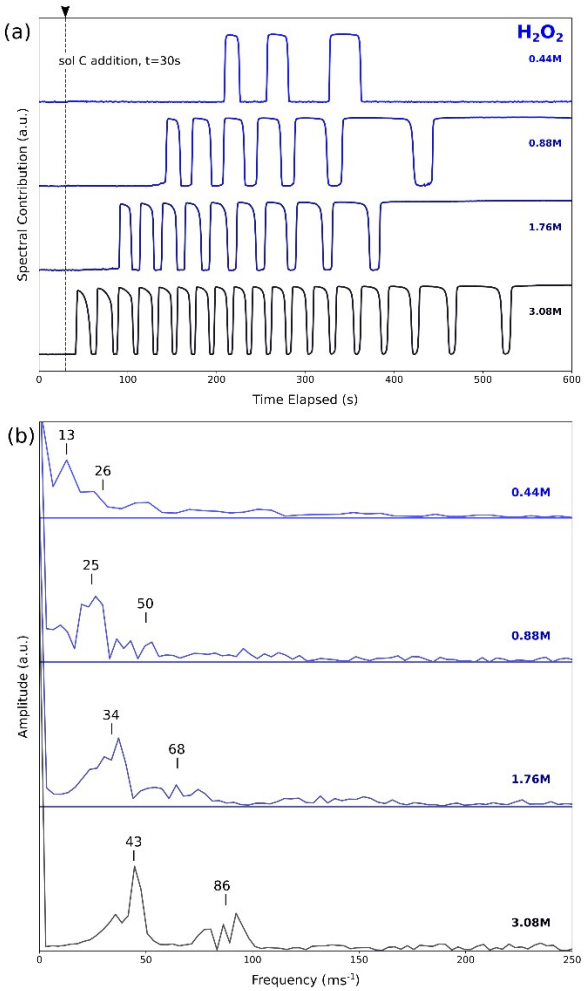

Figure S7: H_2O_2-dependent DCLS spectral contributions following the addition of solution C at (t = 30 s). (a) Time-resolved DCLS signals showing variation in oscillatory behaviour with changing H_2O_2 concentration. (b) Corresponding FFT spectra showing changes in frequency and spectral features with varying H_2O_2 concentration.

Investigating the role of starch in the BR reaction.

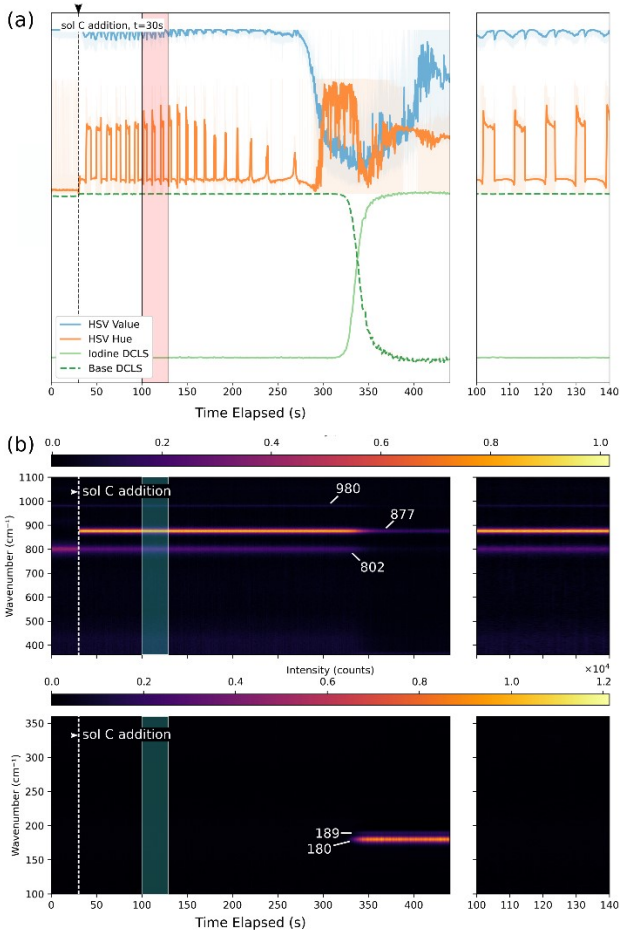

Figure S8: Time-matched BR reaction, (a) showing between final iodine spectral contribution and HSV value for the full BR reaction in the absence of starch, (b) corresponding time-matched in situ Raman spectroscopic time-series BR reaction. Time-matched in situ Raman spectroscopic time-series BR reaction. Time-matched in situ Raman spectroscopic time-series BR reaction.

References

1. Cox, R.A., et al., Resolution of Raman spectra of aqueous sulfuric acid mixtures using principal factor analysis. Canadian Journal of Chemistry, 1981. **59**(17): p. 2591-2598.
2. Rudolph, W.W. and G. Irmer, Raman Spectroscopic Investigation of Speciation in MnSO4(aq). Journal of Solution Chemistry, 2014. **43**(3): p. 465-485.
3. Durig, J.R., O.D. Bonner, and W.H. Breazeale, Raman Studies of Iodic Acid and Sodium Iodate. The Journal of Physical Chemistry, 1965. **69**(11): p. 3886-3892.
4. Ananthanarayanan, V., Raman spectra of single crystals of dicarboxylic acids. Proceedings of the Indian Academy of Sciences - Section A, 1960. **51**(6): p. 328-335.
5. Ramírez-Cedeño, M.L., et al., Fiber Optic Coupled Raman Based Detection of Hazardous Liquids Concealed in Commercial Products. International Journal of Spectroscopy, 2012. **2012**(1): p. 463731.
6. Furrow, S.D. and R.M. Noyes, The oscillatory Briggs-Rauscher reaction. 2. Effects of substitutions and additions. Journal of the American Chemical Society, 1982. **104**(1): p. 42-45.